

Partonic effects on pion interferometry at RHIC

Zi-wei Lin, C.M. Ko, and Subrata Pal

Cyclotron Institute and Physics Department, Texas A&M University, College Station, Texas 77843-3366

Using a multiphase transport (AMPT) model that includes both initial partonic and final hadronic interactions, we study the pion interferometry at the Relativistic Heavy Ion Collider (RHIC). We find that the two-pion correlation function is sensitive to the magnitude of the parton scattering cross section, and a value of about 10 mb is needed to reproduce the measured correlation function in central Au+Au collisions at $\sqrt{s} = 130A$ GeV. The emission source of pions from the AMPT model is non-Gaussian, leading to source radii that can be more than twice larger than the radius parameters extracted from a Gaussian fit to the correlation function.

PACS numbers: 25.75.Gz, 25.75.-q, 24.10.Lx

Particle interferometry based on the Hanbury-Brown Twiss (HBT) effect has long been used to measure the size of an emission source [1]. In heavy ion collisions, it has been suggested that the HBT study can provide information not only on the spatial extent of the emission source but also on its expansion velocity and emission duration [2–5]. In particular, the long emission time as a result of the phase transition from the quark-gluon plasma to hadronic matter in relativistic heavy ion collisions is expected to lead to an emission source which has a much larger radius in the direction of the total transverse momentum of detected two particles (R_{out}) than that perpendicular to both this direction and the beam direction (R_{side}) [5–7]. Since the quark-gluon plasma is expected to be formed in heavy ion collisions at RHIC, it is thus surprising to find that the extracted ratio $R_{\text{out}}/R_{\text{side}}$ from a Gaussian fit to the measured two-pion correlation function in Au+Au collisions at $\sqrt{s} = 130A$ GeV is close to one [8–10]. Also, the extracted radius parameters are small compared to theoretical predictions based on the hydrodynamical model [6]. These experimental results, especially the small value of $R_{\text{out}}/R_{\text{side}}$, have been attributed to strong space-time and momentum correlations in the emission source [11].

In this letter, a multiphase transport model (AMPT) [12–15], that includes both initial partonic and final hadronic interactions, is used to study the pion interferometry in central Au+Au collisions at RHIC at $\sqrt{s} = 130A$ GeV. The AMPT model is a hybrid model that uses the minijet partons from hard processes and the strings from soft processes in the HIJING model [16] as the initial conditions for modeling the collision dynamics. The time evolution of partons is then modeled by the ZPC [17] parton cascade model. At present, this model includes only parton-parton elastic scatterings with an in-medium cross section given by:

$$\frac{d\sigma_p}{d\hat{t}} = \frac{9\pi\alpha_s^2}{2} \left(1 + \frac{\mu^2}{\hat{s}}\right) \frac{1}{(\hat{t} - \mu^2)^2}, \quad (1)$$

where the strong coupling constant α_s is taken to be 0.47, and \hat{s} and \hat{t} are the Mandelstam variables. The effective screening mass μ depends on the temperature and density

of the partonic matter but is taken as a parameter for fixing the magnitude and angular distribution of the parton scattering cross section. After these minijet partons stop interacting, they are combined with their parent strings to fragment to hadrons using the Lund string fragmentation model as implemented in the PYTHIA routine [18]. The final-state hadronic scatterings are then modeled by the ART model [19].

The default AMPT model has been quite successful in describing the measured rapidity distributions of charge particles [13], particle to antiparticle ratios [13], and the spectra of low transverse momentum pions and kaons [14] in heavy ion collisions at SPS and RHIC. Since the initial energy density in Au+Au collisions at RHIC is expected to be much larger than the critical energy density at which the hadronic matter to quark-gluon plasma transition would occur [20,21], the AMPT model has been extended to convert the initial excited strings into partons [15]. In this string melting scenario, hadrons, that would have been produced from string fragmentation, are converted instead to valence quarks and/or antiquarks. Interactions among these partons are again described by the ZPC parton cascade model. The transition of the partonic matter to the hadronic matter is, however, achieved using a simple coalescence model, which combines two nearest partons into mesons and nearest three partons into baryons or anti-baryons. Using parton scattering cross sections of 6-10 mb, the extended AMPT model is able to reproduce both the centrality and transverse momentum (below 2 GeV/c) dependence of the elliptic flow measured in Au+Au collisions at $\sqrt{s} = 130A$ GeV at RHIC [22].

From the AMPT model, the source of emitted particles is obtained from their space-time coordinate x and momentum \mathbf{p} at freezeout, i.e., at their last interactions. Denoting the emission function of the source for pions by $S(x, \mathbf{p})$, the HBT correlation function for two identical pions of momenta \mathbf{p}_1 and \mathbf{p}_2 is then given by [2,23]:

$$C_2(\mathbf{Q}, \mathbf{K}) = 1 + \frac{\int d^4x_1 d^4x_2 S(x_1, \mathbf{K}) S(x_2, \mathbf{K}) \exp[iQ \cdot (x_1 - x_2)]}{\int d^4x_1 S(x_1, \mathbf{p}_1) \int d^4x_2 S(x_2, \mathbf{p}_2)}, \quad (2)$$

where $\mathbf{K} = (\mathbf{p}_1 + \mathbf{p}_2)/2$ and $Q = (\mathbf{p}_1 - \mathbf{p}_2, E_1 - E_2)$. Expecting that the emission function is sufficiently smooth in the momentum space, one can evaluate the correlation function by using \mathbf{p}_1 and \mathbf{p}_2 for \mathbf{K} in the numerator of Eq.(2). Furthermore, the three-dimensional correlation function in \mathbf{Q} is usually shown as a function of the invariant relative momentum ($Q_{\text{inv}} = \sqrt{-Q^2}$) or as a function of the projection of the relative momentum \mathbf{Q} in the “out-side-long” (*osl*) system [3,4], defined by the beam direction (Q_{long}), the direction along the total momentum of the two particles in the transverse plane (Q_{out}), and the direction orthogonal to the above two directions (Q_{side}).

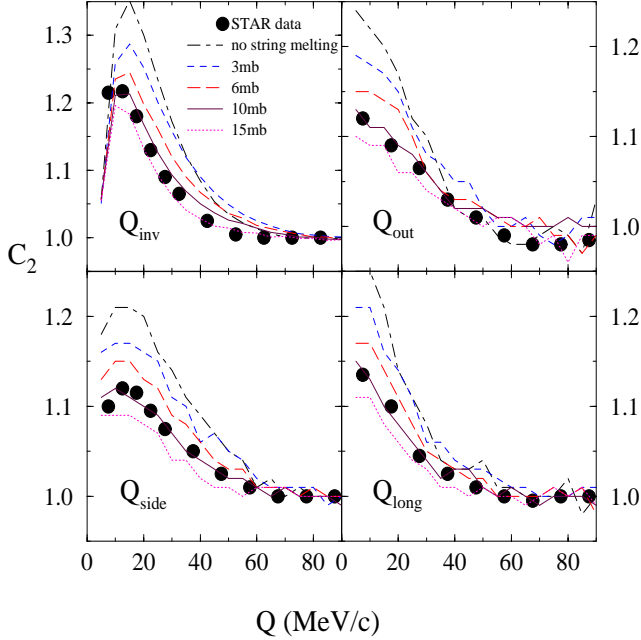


FIG. 1. Correlation functions for midrapidity charged pions with $125 < p_T < 225$ MeV/c. Coulomb correction are shown for the default AMPT model (dash-dotted curves) and for the extended AMPT model with string melting and various values for σ_p . Coulomb-uncorrected correlation functions from the STAR collaboration [22] are shown by filled circles.

Using the emission function obtained from the AMPT model for central ($b = 0$ fm) Au+Au collisions at $\sqrt{s} = 130A$ GeV, we have evaluated the correlation function $C_2(\mathbf{Q}, \mathbf{K})$ in the longitudinally comoving system frame using the program Correlation After Burner [24]. In Fig. 1, we show the one-dimensional projections of the calculated correlation function including final-state Coulomb interaction for midrapidity ($-0.5 < y < 0.5$) charged pions with transverse momentum $125 < p_T < 225$ MeV/c. Also shown are the measured π^- correlation functions from central collisions by the STAR collaboration without removing the effect due to Coulomb interaction [8]. In evaluating the one-dimensional projections of the correlation function onto one of the $Q_{\text{out}}, Q_{\text{side}}$

and Q_{long} axes, we have integrated the other two \mathbf{Q} components over the range $0 - 35$ MeV/c. The dash-dotted curves in Fig. 1 are results from the default

AMPT model (no string melting) with a parton scattering cross section of $\sigma_p = 3$ mb, while other curves in the figure are those from the extended AMPT model with string melting but different values for σ_p . It is seen that with string melting both the width of the Q_{inv} correlation function and its height decrease with increasing σ_p . The decreasing width can be more clearly seen from the calculated correlation functions without including the Coulomb interaction [25], as the value of the correlation function in this case is exactly two at $Q_{\text{inv}} = 0$. Since the integration of the other two \mathbf{Q} components over a fixed range ($0 - 35$ MeV/c) gives a smaller value when the correlation function becomes narrower in \mathbf{Q} , the height of the one-dimensional projection of the correlation function thus decreases with increasing σ_p . To reproduce the measured one-dimensional correlation functions by the STAR collaboration, we find that a parton scattering cross section of about 10 mb is required in the extended AMPT model with string melting.

The size of the emission source can be determined from the emission function via the curvature of the correlation function at $\mathbf{Q} = 0$:

$$R_{ij}(K)^2 = -\frac{1}{2} \frac{\partial^2 C_2(\mathbf{Q}, \mathbf{K})}{\partial Q_i \partial Q_j} \Big|_{\mathbf{Q}=0} = D_{x_i, x_j} - D_{x_i, \beta_j t} - D_{\beta_i t, x_j} + D_{\beta_i t, \beta_j t}, \quad (3)$$

where $x_i (i = 1 - 3)$ denotes the projections of the particle position at freezeout in the *osl* system, i.e., $x_{\text{out}}, x_{\text{side}}$ and x_{long} , and $\beta = \mathbf{K}/K_0$ with K_0 being the average energy of the two particles. In the second line of Eq.(3), we have $D_{x,y} = \langle x \cdot y \rangle - \langle x \rangle \langle y \rangle$, with $\langle x \rangle$ denoting the average value of x . $D_{x,x}$ is thus the variance of the emission function in x , while $\Delta t \equiv \sqrt{D_{t,t}}$ gives the emission duration.

In Fig. 2, we show by solid curves the transverse mass m_T dependence of the source radii R_{out} (upper-left panel), R_{side} (upper-right panel), and R_{long} (lower-left panel) determined from the emission function [22] for midrapidity charged pions given by the AMPT model with string melting and parton cross section of $\sigma_p = 10$ mb for central Au+Au collisions at $\sqrt{s} = 130A$ GeV. Also shown in the lower-right panel by the solid curve is the emission duration Δt obtained from the emission function. It is seen that for $m_T < 0.5$ GeV/c², these radii have values between 7 and 25 fm, and the emission also lasts a long time of more than 20 fm/c.

Since only the correlation function is measured in experiments, the size of emission source is usually estimated by fitting the measured correlation function $C_2(\mathbf{Q}, \mathbf{K})$ with a four-parameter Gaussian function:

$$C_2(\mathbf{Q}, \mathbf{K}) = 1 + \lambda \exp \left(- \sum_{i=1}^3 R_{ii}^2(K) Q_i^2 \right). \quad (4)$$

If the emission source is Gaussian in space-time, then for central heavy ion collisions considered here the radius

parameters obtained from the above Gaussian fit to the correlation function would be the same as those determined directly from the emission function of the source via Eq.(3).

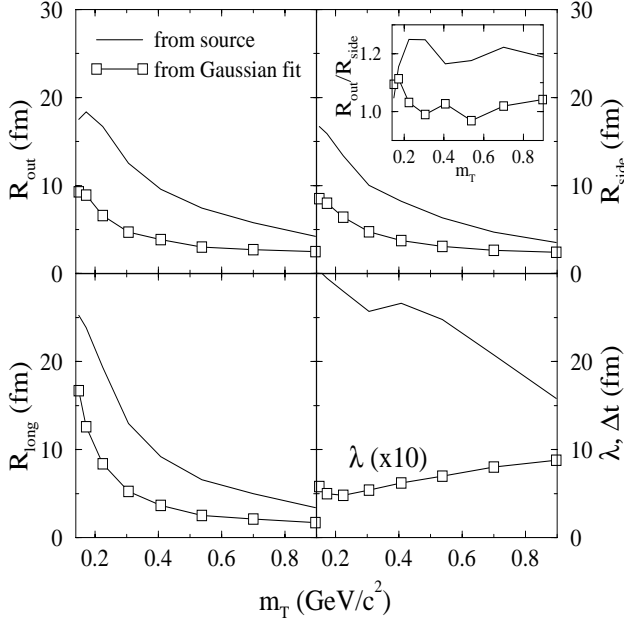


FIG. 2. Source radii and emission duration from the emission function (solid curves), and fitted radius and λ parameters from the Gaussian fit to the correlation function (curves with squares) for midrapidity pions as functions of pion transverse mass m_T . The inset shows the corresponding ratio $R_{\text{out}}/R_{\text{side}}$.

The radius parameters determined from the Gaussian fit to the three-dimensional correlation function in \mathbf{Q} from the AMPT model with string melting and a parton cross section of 10 mb are shown in Fig. 2 by curves with squares as functions of the transverse mass of midrapidity charged pions. For the m_T values shown here, these radius parameters are about a factor of 2 to 3 smaller than the source radii obtained directly from the emission function, shown by the solid curves in the figure. The emission source from the AMPT model thus deviates appreciably from a Gaussian one. The radius parameters from the Gaussian fit to the correlation function have similar values as the experimental ones from fitting the measured correlation function using Eq.(4) [8]. The parameter λ (scaled up by a factor of 10) from the Gaussian fit to the correlation function is shown in the lower-right panel by the curve with squares. It has a value of about 0.5 at low m_T but increases almost to 1 at large m_T . Both the source radii and fitted radius parameters as well as the emission duration obtained from the emission function decrease with increasing m_T . On the other hand, these radii increase with increasing parton scattering cross section as a result of stronger collective expansion of the emission source [25].

Since Eq.(3) gives

$$R_{\text{out}}^2 = D_{x_{\text{out}}, x_{\text{out}}} - 2 D_{x_{\text{out}}, \beta_{\perp} t} + D_{\beta_{\perp} t, \beta_{\perp} t}, \quad (5)$$

and $R_{\text{side}}^2 = D_{x_{\text{side}}, x_{\text{side}}}$, the ratio $R_{\text{out}}/R_{\text{side}}$ contains information about the duration of emission and has been studied extensively [6,8]. This connection between R_{out} and the emission duration becomes clearer if we neglect the $x_{\text{out}} - t$ correlation term $D_{x_{\text{out}}, \beta_{\perp} t}$ in Eq.(5). In the inset of the upper-right panel of Fig. 2, we show the ratio $R_{\text{out}}/R_{\text{side}}$ for midrapidity charged pions. It is seen that the ratio $R_{\text{out}}/R_{\text{side}}$ obtained from the emission function (solid curve) has a value between 1.0 and 1.3 as in predictions based on the hydrodynamical model with freezeout treated via the hadronic transport model [6]. However, with the radius parameters extracted from the Gaussian fit to the correlation function, the ratio $R_{\text{out}}/R_{\text{side}}$ becomes much closer to 1, similar to the experimental values extracted from the measured correlation function [8].

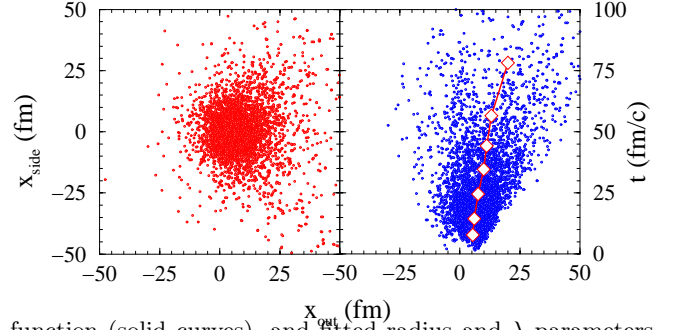


FIG. 3. $x_{\text{out}} - x_{\text{side}}$ (left panel) and $x_{\text{out}} - t$ (right panel) distributions for midrapidity pions with $125 < p_T < 225$ MeV/c from the AMPT model. The curve with open diamonds is the fit to the data.

To investigate the reason for the large difference between the source radii obtained directly from the emission function and from the Gaussian fit to the correlation function, we show in Fig. 3 the $x_{\text{out}} - x_{\text{side}}$ distribution (left panel) and the $x_{\text{out}} - t$ distribution (right panel) at freezeout for midrapidity pions with $125 < p_T < 225$ MeV/c from the AMPT model with string melting and $\sigma_p = 10$ mb. It is seen that the emission source is shifted in the direction of the pion transverse momentum, i.e., $\langle x_{\text{out}} \rangle > 0$. This positive shift in x_{out} results from the collective expansion of the emission source [15].

If the width in x_{out} were much smaller than the average value $\langle x_{\text{out}} \rangle$, the emission source would have a shell-like shape, similar to the emission source with strong opacity introduced in a hydrodynamical model [11]. The emission source also shows a large halo around a central core. The halo consists not only of pions from decays of long-lived resonances such as the ω but also of thermal pions. In calculating the correlation function, we have also included pions from the decay of η resonances as in experiments. Their effects on the radius parameters obtained from the Gaussian fit to the correlation function are thus included. On the other hand, we have excluded these pions in evaluating the source radii from the emission function due to the very long lifetime of η . Since long-lived resonances mainly affect the correlation func-

tion at small relative momenta [26], they are important in determining the λ parameter.

As to the $x_{\text{out}} - t$ distribution of the emission function shown in the right panel of Fig. 3, it has a strong positive $x_{\text{out}} - t$ correlation as clearly seen from the solid curve with open diamonds, which shows that the average value $\langle x_{\text{out}} \rangle$ increases with the freezeout time t . The $x_{\text{out}} - t$ correlation leads to a large positive value for the $x_{\text{out}} - t$ correlation term $D_{x_{\text{out}}, \beta_{\perp} t}$ in Eq.(5), making it difficult to extract information about the duration of emission from the ratio $R_{\text{out}}/R_{\text{side}}$. Similar results have been seen previously in studies based on the RQMD model for heavy ion collisions at SPS [27,28]. We note that the imaging method [29], developed for extracting the emission function of a source from the correlation function, will be very useful for verifying the non-Gaussian features of the emission source in high energy heavy ion collisions.

In summary, we have studied the pion interferometry in relativistic heavy ion collisions at RHIC. Using a multi-phase transport model that includes both initial partonic and final hadronic interactions, we find that the two-pion correlation function is sensitive to the parton scattering cross section. To reproduce the measured correlation function in central Au+Au collisions at $\sqrt{s} = 130A$ GeV requires both the melting of initial strings to partons and a large parton scattering cross section of about 10 mb. We further find that the emission source is non-Gaussian in space and time. It not only shifts significantly to the direction along the pion transverse momentum but also has a strong correlation between this displacement and the freezeout time. Consequently, the source radii extracted directly from the emission function are about a factor of 2 to 3 larger than the radius parameters extracted from a Gaussian fit to the three-dimensional correlation function. Furthermore, the ratio $R_{\text{out}}/R_{\text{side}}$ obtained from the emission function is larger than that extracted from a Gaussian fit to the correlation function, which is found to be close to one. Although the correlation function requires only the space-time information of pions at freezeout, it is shown to be sensitive to the partonic dynamics during the early stage of heavy ion collisions. The study of pion interferometry thus helps to confirm the formation of the partonic matter at RHIC and to study its properties.

We appreciate useful discussions with P. Danielewicz, M. Gyulassy, U. Heinz, M. Lisa, M. Murray, P. Philip, T. Csörgő, S. Pratt, N. Xu, and Q.H. Zhang. This paper is based on work supported by the U.S. National Science Foundation under Grant Nos. PHY-9870038 and PHY-0098805, the Welch Foundation under Grant No. A-1358, and the Texas Advanced Research Program under Grant No. FY99-010366-0081.

-
- [1] R. Hanbury Brown and R.Q. Twiss, *Nature* (London) **178**, 1046 (1956).
 - [2] S. Pratt, *Phys. Rev. Lett.* **53**, 1219 (1984).
 - [3] G. Bertsch, M. Gong and M. Tohyama, *Phys. Rev. C* **37**, 1896 (1988).
 - [4] S. Pratt, T. Csörgő and J. Zimanyi, *Phys. Rev. C* **42**, 2646 (1990).
 - [5] D. H. Rischke and M. Gyulassy, *Nucl. Phys. A* **608**, 479 (1996).
 - [6] S. Soff, S. A. Bass and A. Dumitru, *Phys. Rev. Lett.* **86**, 3981 (2001).
 - [7] S. Soff, S. A. Bass, D. H. Hardtke and S. Y. Panitkin, *Phys. Rev. Lett.* **88**, 072301 (2002); nucl-th/0202019.
 - [8] C. Adler *et al.*, STAR Collaboration, *Phys. Rev. Lett.* **87**, 082301 (2001).
 - [9] S. C. Johnson, PHENIX Collaboration, *Nucl. Phys. A* **698**, 603 (2002).
 - [10] K. Adcox *et al.*, PHENIX Collaboration, nucl-ex/0201008.
 - [11] B. Tomasik and U. W. Heinz, nucl-th/9805016.
 - [12] B. Zhang, C. M. Ko, B. A. Li and Z. W. Lin, *Phys. Rev. C* **61**, 067901 (2000).
 - [13] Z. W. Lin, S. Pal, C. M. Ko, B. A. Li and B. Zhang, *Phys. Rev. C* **64**, 011902 (2001).
 - [14] Z. W. Lin, S. Pal, C. M. Ko, B. A. Li and B. Zhang, *Nucl. Phys. A* **698**, 375 (2002).
 - [15] Z. W. Lin and C. M. Ko, *Phys. Rev. C* **65**, 034904 (2002).
 - [16] X. N. Wang and M. Gyulassy, *Phys. Rev. D* **44**, 3501 (1991).
 - [17] B. Zhang, *Comput. Phys. Commun.* **109**, 193 (1998).
 - [18] T. Sjostrand, *Comput. Phys. Commun.* **82**, 74 (1994).
 - [19] B. A. Li and C. M. Ko, *Phys. Rev. C* **52**, 2037 (1995).
 - [20] D. Kharzeev and M. Nardi, *Phys. Lett. B* **507**, 121 (2001).
 - [21] B. Zhang, C. M. Ko, B. A. Li, Z. W. Lin and B. H. Sa, *Phys. Rev. C* **62**, 054905 (2000).
 - [22] K. H. Ackermann *et al.*, STAR Collaboration, *Phys. Rev. Lett.* **86**, 402 (2001).
 - [23] U. A. Wiedemann and U. W. Heinz, *Phys. Rept.* **319**, 145 (1999).
 - [24] S. Pratt *et al.*, *Nucl. Phys. A* **566**, 103C (1994).
 - [25] Z. W. Lin, C. M. Ko, and Subrata Pal, in preparation.
 - [26] T. Csörgő, B. Lorstad and J. Zimanyi, *Z. Phys. C* **71**, 491 (1996).
 - [27] J. P. Sullivan *et al.*, *Phys. Rev. Lett.* **70**, 3000 (1993).
 - [28] D. E. Fields, J. P. Sullivan, J. Simon-Gillo, H. van Hecke, B. V. Jacak and N. Xu, *Phys. Rev. C* **52**, 986 (1995).
 - [29] D. A. Brown and P. Danielewicz, *Phys. Lett. B* **398**, 252 (1997); *Phys. Rev. C* **57**, 2474 (1998); *ibid* **64**, 014902 (2001).